Extension of the Liège Intra Nuclear Cascade model to light ion-induced collisions for medical and space applications

2013 J. Phys.: Conf. Ser. 420 012065

(http://iopscience.iop.org/1742-6596/420/1/012065)

Journal of Physics: Conference Series **420** (2013) 012065 doi:10.1088/1742-6596/420/1/012065

Extension of the Liège Intra Nuclear Cascade model to light ion-induced collisions for medical and space applications

S. Leray[1], D. Mancusi[1], P. Kaitaniemi[1,3], J.C. David[1], A. Boudard[1], B. Braunn[1], J. Cugnon[2]

[1]CEA/Saclay, Irfu/SPhN, 91191 Gif-sur-Yvette, Cedex, France
[2]University of Liège, AGO Department, allée du 6 août 17, Bât. B5, B-4000 Liège 1, Belgium
[3]Helsinki Institute of Physics, Helsinki, Finland

E-mail: sylvie.leray@cea.fr

Abstract. The Liège Intranuclear Cascade model, INCL4, has been developed to describe spallation reactions, i.e. nucleon and light charged particle induced collisions in the 100 MeV – 3 GeV energy range. Extensive comparisons with experimental data covering all possible reaction channels have shown that, coupled to the ABLA07 de-excitation code from GSI, it is presently one of the most reliable models in its domain. Recently, the treatment of composite particle as projectlies has been revisited mainly to improve predictions related to secondary reactions in spallation targets. An example regarding astatine production in LBE targets will be shown. Also, the model has been extended to light ion (up to oxygen) induced reactions, mostly for medical and space application purposes. This version is available in GEANT4. The first results indicate that the model agrees at least as well as other models with experimental data. In this paper, the different assumptions and ingredients of the model will be presented and comparisons with relevant experimental data will be shown. The sensitivity to the de-excitation stage is also discussed.

1. Introduction

The Liège Intranuclear Cascade model, INCL4 [1], has originally been developed to describe spallation reactions, i.e. nucleon and light charged particle induced collisions in the 100 MeV – 3 GeV energy range. Coupled to the ABLA de-excitation code from GSI [2], it has been extensively compared with experimental data covering all possible reaction channels and continuously improved during the last ten years, part of the work being done in the framework of the HINDAS [3] FP5 and EUROTRANS/NUDATRA [4] FP6 EC projects, whose objective was to provide improved simulation tools for the design of ADS transmuters. The combination of versions developed in this framework, INCL4.5 [5] and ABLA07 [6], has been shown [7] to be one of the models giving the best overall agreement with experimental data in the benchmark of spallation models organized recently under the auspices of IAEA [8]. Different versions of INCL4, alone or coupled to ABLA, have been provided for implementation into various high-energy transport codes : MCNPX [9], GEANT4 [10] and more recently PHITS [11] and MARS [12].

The main motivations for the work on spallation reaction models were the development of spallation neutron sources and projects of accelerator-driven sub-critical reactors and of

radioactive ion beam facilities. However, other applications of high energy reactions involving light-ion induced reactions are nowadays raising a lot of interest: for instance hadrontherapy, radioprotection of astronauts and radiation damage to microelectronics circuits near accelerators or in space missions, and simulation of detector set-ups in nuclear and particle physics experiments.

There is an increasing number of hadrontherapy facilities in Asia and in Europe that use or plan to use carbon beams around a few hundreds of MeV/u to irradiate deep-seated radio-resistant cancerous tumors. The fragmentation of the carbon ion along its path to the tumour produces secondary neutrons and charged particles. This is a subject of concern because of potential and undesirable long-term effects which may restrain the development of this therapy, up to now used only when other techniques fail. Also, the application of positron emission tomography (PET) techniques for in-vivo range verification [13] relies on an accurate estimate of the production and of the stopping-site distribution of the β^+ emitters, ^{10}C and ^{11}C. Only high-precision Monte-Carlo calculations can provide a reliable relation between the dose-deposition and the β^+-activity distributions. There is therefore a need for transport codes able to predict reliably carbon fragmentation and to provide correlations among different observables — which is beyond the applicability of deterministic models.

In space, irradiation is due galactic cosmic radiation composed of ions from protons to iron with an energy distribution peaking around 1 GeV per nucleon. As shown in [14], although heavy ions are far less frequent in cosmic radiation than protons, they are responsible for the major part of the dose received by the space crew. Damage to electronic devices in space is also becoming an important issue. In order to accurately simulate these effects, models for the reactions occurring in the vessel structure and in biological tissues (for instance Fe+C reactions) should obviously be reliable since they produce secondary nuclei.

Because of the growing interest in these types of applications, most of the high-energy transport code are being extended to heavy-ion transport or, if this option was already available, more attention is paid to the quality of the implemented nuclear reaction models. For instance, the MCNPX team has recently begun to upgrade it to heavy-ion transport [15] and a benchmarking of GEANT4 for medical applications is regularly organized. This is why the extension of the INCL4 model to light-ion (up to ^{18}O) has recently been undertaken. This work has actually begun with the possibility of handling composite projectiles in the standard model. The treatment of projectiles up to alphas have been revisited [16], especially at low incident energies, in order to correctly predict secondary reactions in spallation targets. Examples of results that can be obtained [17] are given in the first part of this paper. In the second part, we briefly describe how the INCL4 model is being extended to light-ion induced reactions and compare it with some available experimental data. Finally, examples of simulation of experimental data relevant for hadrontherapy are given using the model, in its C++ version, implemented in GEANT4.

2. Composite particle induced reactions

Although from the origin, the INCL4 model was designed to handle reactions with light-charged particles up to alpha, little attention had been paid to those up to recently. However, in nucleon-induced reactions high-energy composite nuclei are produced, which are responsible for secondary reactions in a spallation target. Since some of the isotopes produced in secondary reactions can be of concern for radioprotection issues, it is important to have a model able to correctly predict both composite particle production in spallation reactions and low-energy secondary reactions.

2.1. Cluster production in INCL

As regards composite particle production, only models having a specific mechanism to produce high-energy clusters of nucleons during the cascade stage can aspire reproducing the

experimentally observed high-energy tail in composite particle spectra, which cannot be ascribed to the evaporation stage. In INCL4 a mechanism based on surface coalescence in phase space has been introduced in Ref. [18]. It assumes that a cascade nucleon ready to escape at the nuclear surface can coalesce with other nucleons close enough in phase space and form a cluster that will be emitted if its energy is sufficient to overcome the Coulomb barrier. All possible clusters are formed and the priority is given to the one with the lowest excitation energy per nucleon. In later versions of the models, the mechanism, originally limited to $A \leq 4$, has been extended to clusters up to mass 8 and the phenomenological parameters of the model, which include the volume of the phase space cell in which nucleons should be to form a cluster and the distance from the surface at which the clusters are built, have been revisited. Generally, a very good agreement is obtained with experimental data [19]. It should be stressed however that, like all the ingredients and parameters of INCL4, once chosen, the coalescence parameters are kept constant whatever the system studied.

2.2. Treatment of composite particle induced reactions

Secondary reactions occur at low energies, generally below the alleged theoretical limit of validity of INC models. However, when models are implemented into transport codes and used for a large variety of applications, since no better solution exists (data libraries are not available for helium-induced reactions), it is necessary to ensure that the model predicts at least the gross features of all possible interactions. This is why an effort has been devoted to improve the treatment of low-energy composite particle induced reactions in INCL4. Details of the modifications brought to the model are discussed in [16].

In the original version, an incident cluster was considered as a collection of independent on-shell nucleons with internal Fermi motion superimposed to the collective motion. This approximation is justified at high energy, but it is not really appropriate for reactions at low incident energy, when binding energy and Fermi energy are not small quantities compared with the incident kinetic energy. Therefore, the model has been modified adding the following ingredients:

(a) the composite projectile is described as a collection of off-shell independent nucleons with Fermi motion, ensuring full energy and momentum conservation;

(b) geometrical spectators, i.e. nucleons not passing through the target volume, are put on-shell and the energy needed to preserve a correct balance is taken from the participant nucleons;

(c) if one of the nucleons tries to enter into the target below the Fermi level, all nucleons are absorbed leading to a complete fusion reaction as detailed below;

(d) the projectile Coulomb deviation is now explicitely taken into account;

(e) experimental mass tables instead of average values, which were sufficient at high energies but were problematic close to reaction thresholds, are used, ensuring correct Q-values for the different reaction channels.

At very low energy, the nuclear reaction proceeds by a total absorption of the projectile and the formation of a compound nucleus which will then decay. To account for this, we have introduced a smooth empirical description of the transition between the full absorption and the usual intra nuclear cascade regime (actually only for projectiles with $A \leq 4$) in the following way: The projectile content in terms of nucleons and the Coulomb deviation is treated as before, but the energy of individual nucleons can be negative and sometimes even below the Fermi level in the target nucleus (see Fig. 1), a situation hardly acceptable in the cascade picture. Nucleons missing the sphere of calculation are kept as individual nucleons and put on shell. The necessary energy for this is equally taken from all nucleons entering in the sphere ("participants"). If a participant has an energy lower than the target Fermi level and crosses the core of the target

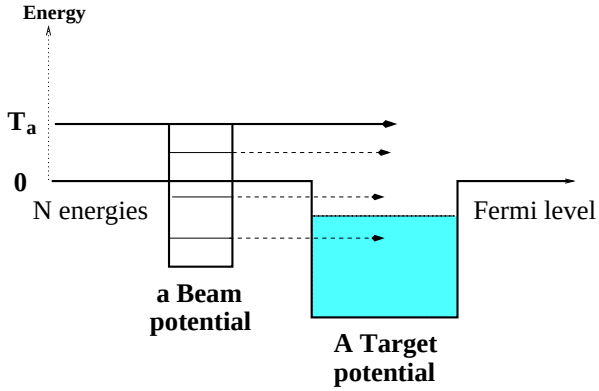

Figure 1: Scheme of the absorption mechanism in composite particle induced reactions.

density, a compound nucleus is produced and treated by the de-excitation has the usual remnant nucleus of the cascade. There is no more "cascade" calculation in that case.

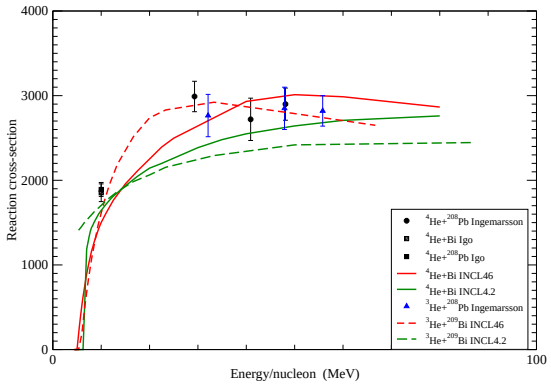

Figure 2: Total reaction cross sections as a function of incident energy for alphas (solid lines) and ^3He (dashed lines) on Bi calculated with INCL4.6-ABLA07 (red curves) and the older version INCL4.2-ABLA (green curves) compared to experimental data on Pb and Bi targets from [20, 21, 22]

With these modifications, the model is able to predict rather well helium-induced total reaction cross-sections [16], as can be seen in Fig. 2, in which it is compared to available experimental data [20, 21, 22] and to the predictions of the original version. It also reproduces reasonably well the different reaction channels that opens with increasing incident energy. This is illustrated in Fig. 3, which shows experimental cross sections, found in the EXFOR experimental nuclear reaction database [23], regarding $^{209}Bi(\alpha, xn)$ for different x values, as a function of the incident particle kinetic energy, compared with the model.

This success may seem surprising since INC models are not supposed to be used to describe reactions below $\sim$ 150 MeV and even less fusion reactions. Actually, this can be understood if one realizes that the model has by construction correct macroscopic properties, thanks to the realistic phase-space densities and to the Coulomb deviation, and that, once nucleons have entered into the target nucleus, they are mostly trapped within the nuclear potential (especially thanks to our absorption procedure) and not sensitive to the detail of the intranuclear cascade. Our model obviously contains some phenomenology but probably not more than many fusion models available on the market, with the advantage that, when the incident energy increases, the model can naturally describe the transition from complete to incomplete fusion.

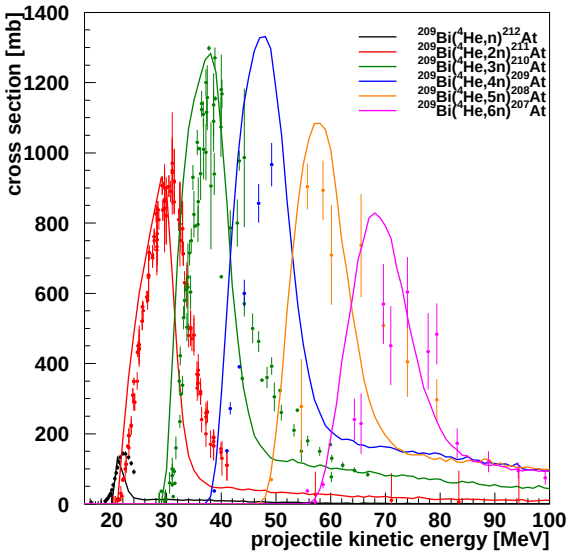

Figure 3: $^{209}Bi(\alpha, xn)$ cross sections for $x = 1$ to 6 as functions of the α incident kinetic energy. The red curves correspond to the predictions of the INCL4.6+ABLA07 model. The experimental data were compiled using the experimental nuclear reaction database, EXFOR [23]

It should be mentioned however that, although still acceptable, the agreement is less good in the case of ^{3}He (not seen here), in particular for $1n$ and $2n$ channels. This is ascribed in [16] to the fact that ^{3}He is less bound and its possible dissociation is not well handled by the model. In addition, our fusion criteria may be less appropriate in this case.

2.3. Application to astatine production in liquid lead-bismuth targets

An example of possible application of our model is the prediction of astatine production in a liquid lead-bismuth(LBE) target. In [17], the model, implemented in MCNPX [24], has been used to simulate the results measured by the ISOLDE IS419 experiment in Ref. [25]. The atomic charge ($Z = 85$) of astatine is larger than that of bismuth by two units. This means that it can be produced only through ($Z = 1, \pi^{-}$) reactions on bismuth or via secondary reactions involving $Z \geq 2$ particles. Fig. 4 shows the global production rate of the different astatine isotopes and the contributions from the different possible mechanisms. It appears that the heaviest isotopes are produced only through secondary helium-induced reactions. On the other hand, both mechanisms populate the other isotopes, the very lightest ones preferentially originating from double charge exchange reactions.

Fig. 5 shows total production yields of astatine isotopes measured in the ISOLDE target compared with the result of INCL4.6-ABLA07 (solid red line) and the former version of the model (blue line) included in MCNPX. The isotopes produced in the target by MCNPX have been passed through CINDER'90 evolution code [26] in order to take into account the actual irradiation and measurement history. For the normalization, a complete release of astatine is assumed. A remarkable agreement between the new calculation and the experiment is observed, regarding not only the shape of the isotopic distribution but also the absolute release rates. Clearly all the new features discussed in the preceding sections, in particular the better handling of low energy helium-induced reactions, have considerably improved the predictive capability of our model.

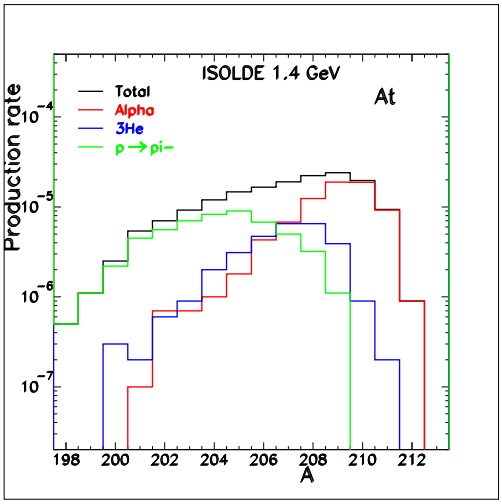

Figure 4: The different reaction channels contributing due to production of astatine isotopes as predicted by INCL4.6-ABLA07 implemented into MCNPX for the ISOLDE LBE target irradiated by 1.4 GeV protons: black total production, green: production through (p, π^-) reactions; red and blue: through secondary reactions induced by alphas and ^3He respectively.

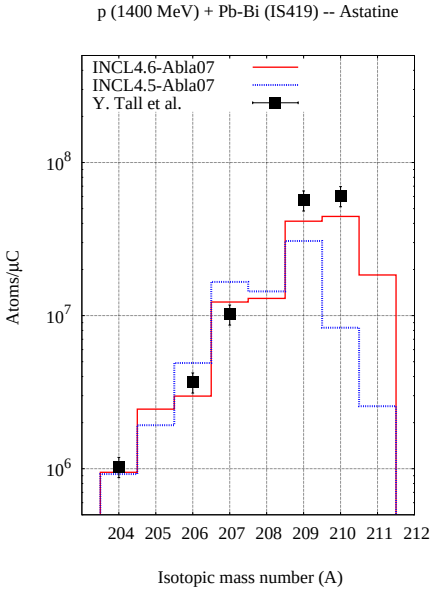

Figure 5: Astatine release rates measured by Tall et al. [25] at 1.4 GeV compared to MCNPX simulations, taking into account the actual irradiation and measurement history through the CINDER'90 evolution code, using INCL4.6-ABLA07 (red line) or INCL4.5-ABLA07 (dashed blue line).

3. Light-ion induced reactions

As already said in the introduction, the idea to extend our model to heavy-ion reactions has arisen from the need of predictive transport codes for applications such as hadrontherapy and space radiation protection. Since the model is very successful in nucleon and composite particle induced reactions, it seemed natural to try to extend it to heavier projectiles. It is clear that our model cannot aspire to describe collisions of two very heavy nuclei since it does not have physics ingredients allowing for instance the prediction of important collective effects. Therefore, we

have limited the extension to ^{18}O projectiles. The goal is to provide an event-generator for high-energy transport codes, able to calculate the characteristics of all particles and nuclei generated in a particular application, with a main focus on hadrontherapy.

3.1. The model

The first INCL light ion extension [27, 28], based on the INCL4.2 version of the nucleon-induced reaction model, consisted of two main parts: handling of the projectile as a collection of individual nucleons and de-excitation of the projectile fragments after the reaction. The main cascade in the target nucleus is treated following the standard INCL cascade procedure as described in Ref. [1]. This version, translated to C++ and coupled with ABLA, has been included in GEANT4 [29]. In this approach, clearly the target and projectile are not treated symmetrically. If we try to interpret the reaction in the framework of a participant-spectator picture, the treatment of the target spectator and participant zone (where NN collisions happen) is satisfactory while the projectile spectator is obviously not correctly handled. When one is interested in fragments of the projectile, this deficiency is circumvented by reversing the reaction (i.e. the target impinging on the projectile) and then boosting it back to the laboratory frame.

Recently, the model has been revisited on the basis of the INCL4.6 version and totally rewritten in C++. This light-ion extended version is denoted as INCL++. The version shown in this paper is v5.1 and has been distributed with the latest GEANT4 beta release (v9.6β).

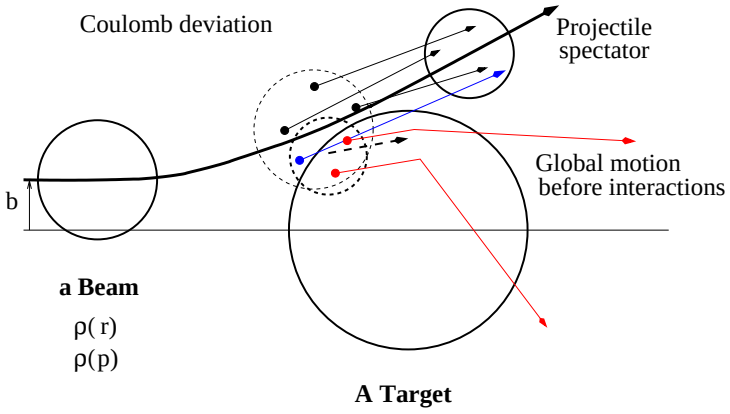

Figure 6: Scheme of a Nucleus-Nucleus collision in INCL++ v5.1.

Let us briefly describe its main features. The ion comes from infinity at a random impact parameter (see Fig. 6). It is described as a bulk of (N, Z) nucleons in the ion rest frame whose positions and momenta are randomly chosen in a realistic r and p space density (gaussian). A constraint is applied to have the vectorial sum equal to zero in both spaces. For each configuration the depth of a binding potential is determined so that the sum of the nucleon energies is equal to the tabulated mass of the projectile nucleus. A Lorentz boost with the projectile velocity is applied to the nucleon quadrivectors to define them in the laboratory system (target at rest). The nucleons are no more on mass shell but the sum of energies and vector momenta are correct. The ion follows globally a classical Coulomb trajectory until one of its nucleon impinges on a sphere of calculation around the target nucleus, large enough to marginally neglect nuclear interactions. Considering the collective cluster velocity, some of the nucleons will never interact with this sphere and will be combined together in the "projectile spectator". All other nucleons are entering the calculation sphere. They move globally (with

the beam velocity) until one of them interacts, being close enough to a target nucleon. The NN interaction is then computed with the individual momenta, and Pauli blocking is tested. Nucleons crossing the sphere of calculation without any NN interaction are also combined in the "projectile spectator" at the end of the cascade.

The projectile spectator nucleus is kinematically defined by its nucleon content and its excitation energy obtained by an empirical particle-hole model based on the energy configuration of the current projectile and the removed nucleons (interacting with the target). This nucleus is then given to a de-excitation model. It is quite clear that this "projectile spectator" has not received any explicit contribution from the zone of interaction which is entirely contained in the target remnant with two consequences: the calculation is not symmetric and the residue of the target should be more realistic than the "projectile spectator" at this stage of the model. In this model, energy and momentum are always conserved.

3.2. Comparison with experimental data

In order to compare with experimental data, the INC model has to be coupled to a de-excitation model. Our standalone version has been coupled to the ABLA07 model [6], as the INCL4.6 fortran model. In GEANT4, it is linked with the native de-excitation handler [30]. This handler, depending on the mass and the excitation energy of the excited nuclei provided by the cascade, chooses between three different statistical de-excitation models (a Fermi break-up model, an evaporation model or a multifragmentation model) to bring back the nuclei to their fundamental state. This allows comparing the respective merits of ABLA07 and GEANT4 de-excitation.

The calculation is still not symmetric although the projectile spectator is better treated than in the first version of our model. This means that, depending on the observable that one is interested in, the calculation should be done either in direct or in inverse kinematics. In the following section, in which we compare the model with some experimental data, we show both choices of kinematics in the case of the symmetric system $^{12}C +^{12} C$ to emphasize the resulting differences.

Comparisons are also done with other models available in GEANT4: the binary cascade (BIC) from Folger *et al.* [31] and in some cases the GEANT4 Quantum Molecular Dynamic model (QMD) developed by Koi [32]. Both are linked to the GEANT4 de-excitation handler.

3.2.1. Neutron production The first results that we compared are neutron production cross-sections measured in the $^{12}C +^{12} C$ system at 135 and 290 MeV by Sato *et al.* [33] and Iwata *et al.* [34], respectively. In Fig. 7, calculations done using either inverse or direct kinematics are plotted. High energy neutrons in direct kinematics are mostly arising from NN collisions in the INC model plus neutrons from the de-excitation of the projectile spectator, while in inverse kinematics they result from the de-excitation of the target remnant or are the low energy partner in NN collisions. Globally the inverse kinematics gives a better agreement except at 135 MeV at very forward angles.

Fig. 8 shows the comparison of the data with the present model, the former version INCL4.2, both in inverse kinematics, and BIC, all models being coupled to the GEANT4 de-excitation handler. It can be observed that the new version of our model better reproduces the data than the former version and that BIC is definitely less good.

Finally, in Fig. 9 we present results using two different de-excitation models, ABLA07 and the GEANT4 de-excitation, coupled to INCL++, here in the direct kinematics case. The results are not very different except at low neutron energies, corresponding to neutrons from the de-excitation of the target remnant, where ABLA07 seems better.

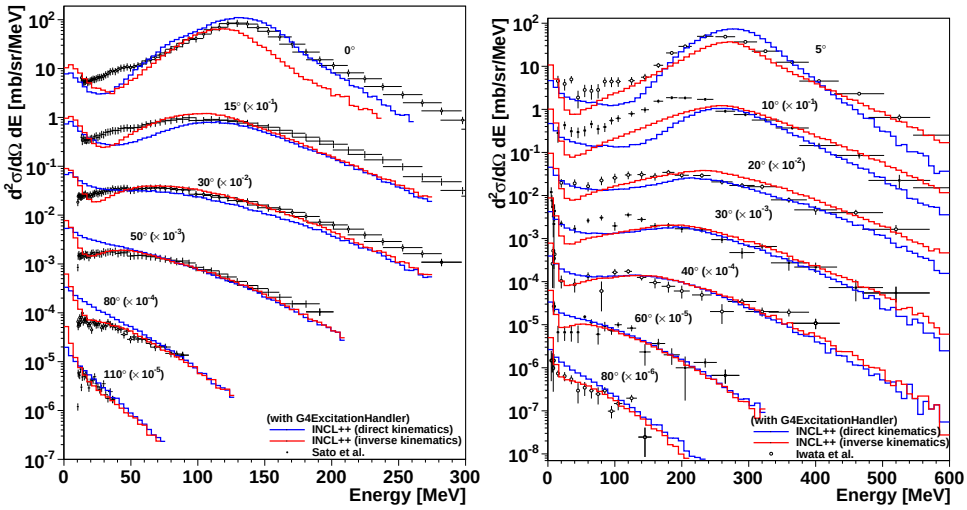

(a) $^{12}C +^{12} C$ 135 MeV/u (b) $^{12}C +^{12} C$ 290 MeV/u

Figure 7: Neutron production double differential cross sections in the $^{12}C +^{12} C$ system at 135 MeV/u [33] and 290 MeV/u] [33] compared to INCL++ in GEANT4 in direct and inverse kinematics.

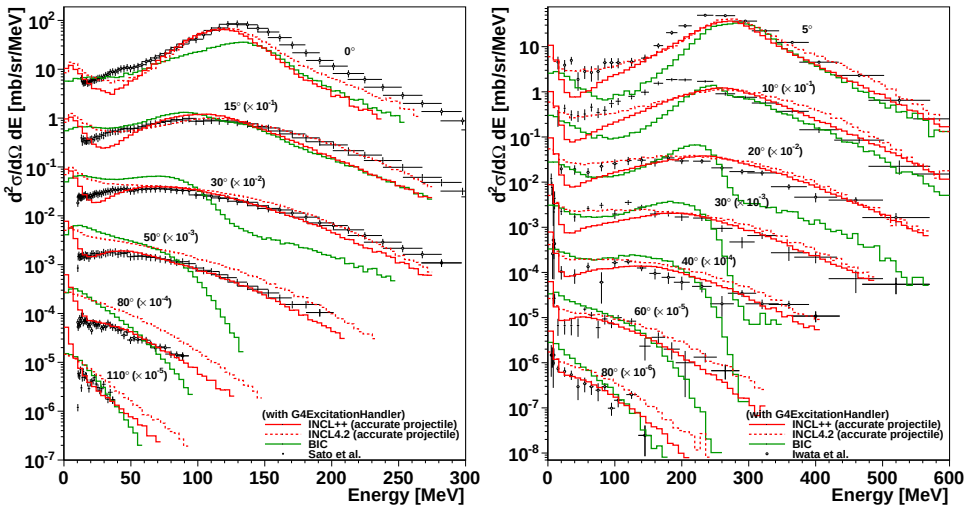

(a) $^{12}C +^{12} C$ 135 MeV/u (b) $^{12}C +^{12} C$ 290 MeV/u

Figure 8: Same as Fig. 7 but the data are compared to INCL++ and INCL4.2, both in inverse kinematics, and BIC, all INC coupled to the GEANT4 de-excitation handler.

3.2.2. Charge changing cross-sections Results on residue production are generally more sensitive to details of the models. In Fig. 10 several sets of data concerning charge changing cross-sections from Ref. [35] are compared to our model, present and former versions, and to BIC. The experiment was devoted to the study of projectile fragmentation on a carbon target. Since the model is available only up to oxygen projectiles, the calculations have been performed in inverse kinematics. As said before, we expect our model to be better for the target remnant, i.e precisely for projectile fragments in inverse kinematics. Generally, our model gives a better

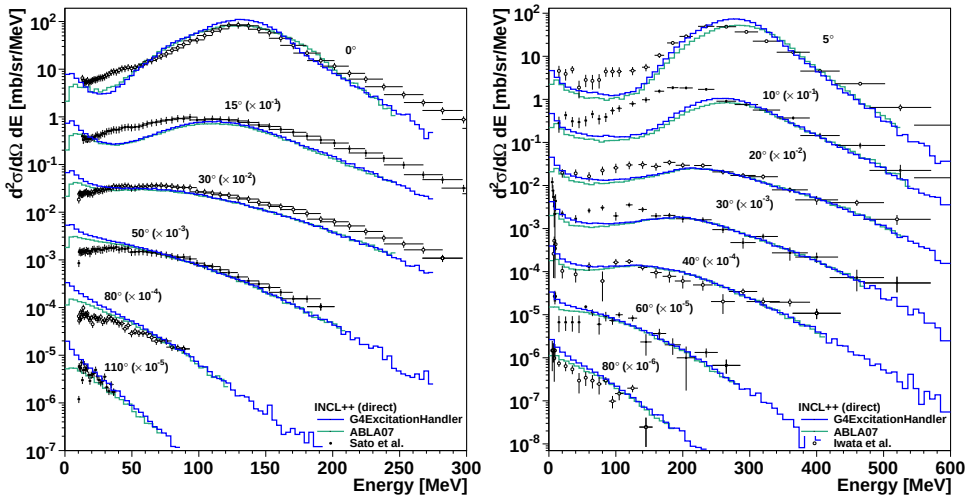

(a) $^{12}C +^{12} C$ 135 MeV/u (b) $^{12}C +^{12} C$ 290 MeV/u

Figure 9: Same as Fig. 7 but the data are compared to INCL++ coupled to two different de-excitation models, ABLA07 and GEANT4 de-excitation handler.

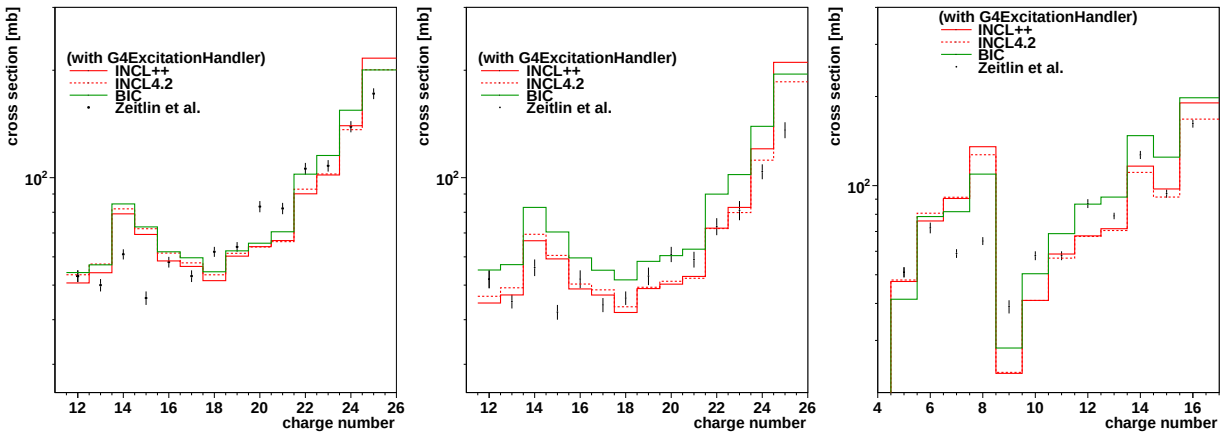

(a) $^{56}Fe +^{12} C$ 500 MeV/u (b) $^{56}Fe +^{12} C$ 3000 MeV/u (c) $^{35}Cl +^{12} C$ 500 MeV/u

Figure 10: Charge changing cross-sections from Ref. [35] compared with INCL++, INCL4.2 and BIC.

agreement with the data than BIC. However, some significant discrepancies can be noticed, especially for the lightest residues.

We have also compared the effect of the choice of the de-excitation model. This can be seen in Fig. 10. Clearly the results are largely dependent on the choice: the GEANT4 de-excitation gives the best fit to the experimental data while ABLA07 has a problem in predicting light nuclei. This may be due to the fact that the model was up to now mainly tested, and therefore adjusted, on systems with excitation energies much smaller than the values reached in the cases studied here.

3.3. Simulations of thick targets

With the model implemented into GEANT4, it is possible to perform simulations of experiments done with thick targets. In Fig. 12, double-differential cross sections of different charged particles

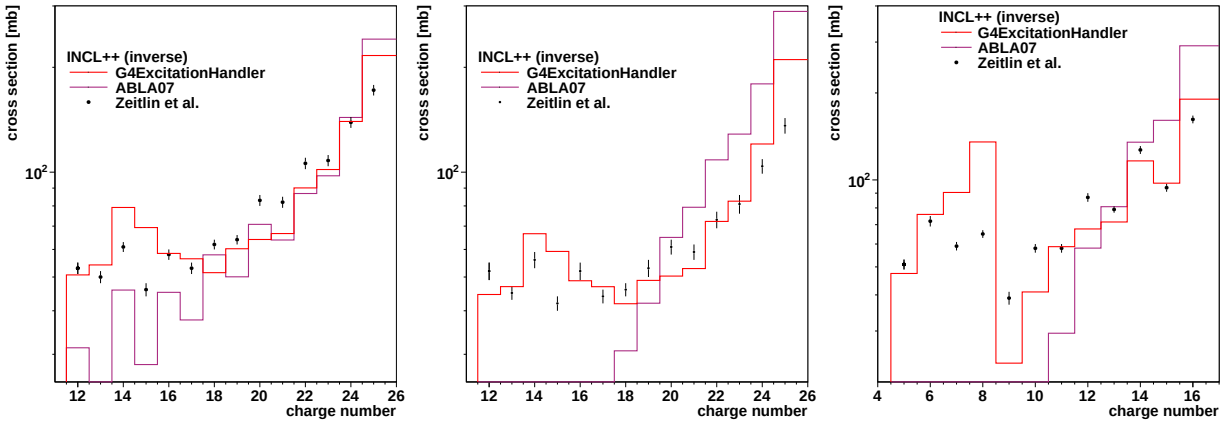

(a) $^{56}Fe +^{12} C$ 500 MeV/u (b) $^{56}Fe +^{12} C$ 3000 MeV/u (c) $^{35}Cl +^{12} C$ 500 MeV/u

Figure 11: Charge changing cross-sections from Ref. [35] compared with INCL++ coupled to two different de-excitation models, ABLA07 and GEANT4 de-excitation handler.

produced by a 200 MeV/u ^{12}C beam stopped in 12.78 cm of water (from Gunzert-Marx *et al.* [36]) are compared to calculations done with GEANT4 using either INCL++ or QMD. Our model agrees very well with the proton data, both in shape and level of cross-sections. QMD is slightly less good. For deuterons and alphas, the data could not be reproduced without a global renormalization, whatever the model. Once renormalized, our model satisfactorily reproduces the data.

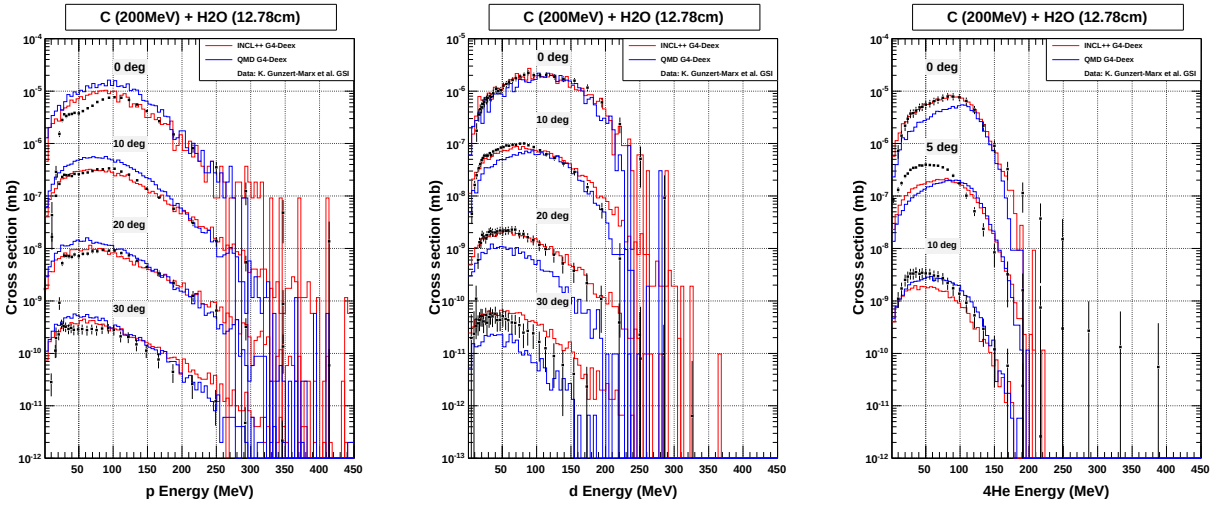

(a) protons (b) deuterons (c) alphas

Figure 12: Double-differential cross sections of protons (a), deuterons (b) and alphas (c) produced by a 200 MeV/u ^{12}C beam stopped in 12.78 cm of water (from Gunzert-Marx *et al.*[36])

Other thick target simulations have been done. They concern the data presented at this

conference by B. Braunn *et al.* [37], in which nuclear charge distributions from the fragmentation of a ^{12}C beam at 95 MeV/u as projectile have been measured with different thicknesses of PMMA targets [38]. We here only show the comparison of production rates for the 5 *mm* target at three different angles. It can be observed that our model reproduces rather well the light ion cross-sections (up to $Z = 4$) but tends to underestimates higher charges at forward angles while BIC overestimates these elements at 10° and 20°. QMD seems to give globally a slightly better agreement with the data.

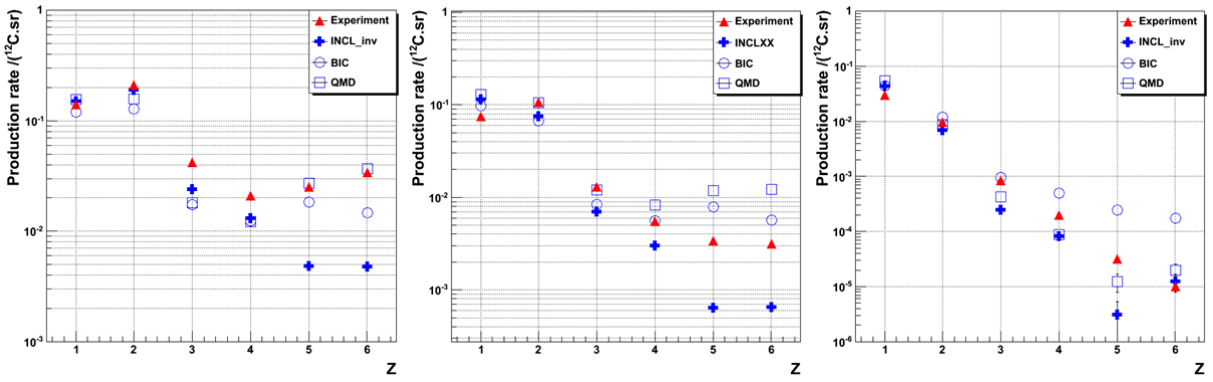

(a) 7 degrees (b) 10 degrees (c) 20 degrees

Figure 13: Nuclear charge distributions at different angles from a ^{12}C beam at 95 MeV/u interacting with a 5 mm PMMA target. The results from the three different models: INCL++ (blue crosses), BIC (blue circles) and QMD (blue squares), are compared to the experimental data (red triangles) from Braunn *et al.*[38].

4. Conclusion

We have presented in this paper recent extensions of the Liège Intranuclear Cascade model, INCL4, which was originally developed to describe nucleon and light charged particle induced reactions in the 100 MeV – 3 GeV energy range. They regard first a revisiting of reactions involving composite particles at low incident energies motivated mainly by the need to correctly account for secondary reactions in spallation targets. Second, the model has been extended to light ion induced collisions with projectiles up to ^{18}O keeping its main features. Although the treatment of target and projectile is not fully symmetric, but provided that the model is used with the kinematics (direct or inverse) most appropriate to the considered observables, it gives very satisfactory results when compared to different sets of experimental data. Being included in GEANT4, it can be used to simulate thick target problem and gives results generally better than BIC and comparable or only slightly less good than QMD, but with a much shorter CPU time. Further improvements, in particular to make the model symmetrical for projectile and target, are under progress.

5. References

[1] Boudard A, Cugnon J, Leray S and Volant C, 2002 Phys. Rev. **C 66**, 044615.
[2] Junghans A R *et al.*, 1998 Nucl. Phys. **A 629**, 635.
[3] HINDAS. EC contract FIKW-CT-2000-00031, Final report. ed. J.P. Meulders, A. Koning and S. Leray, 2005.
[4] FP6 Euratom project EUROTRANS/NUDATRA, 2004 EC contract number FI6W-CT-2004-516520.
[5] Boudard A and Cugnon J, 2008 Proceedings of the Joint ICTP-IAEA Advanced Workshop on Model Codes for Spallation Reactions, ICTP Trieste, Italy, 4-8 February 2008, D. Filges, S. Leray, Y. Yariv, A. Mengoni,

A. Stanculescu, and G. Mank Eds., IAEA INDC(NDS)-530, Vienna, August 2008, p29. http://www-nds.iaea.org/reports-new/indc-reports/indc-nds/indc-nds-0530.pdf
[6] Kelic A, Ricciardi M V and Schmidt K H, 2008 Proceedings of the Joint ICTP-IAEA Advanced Workshop on Model Codes for Spallation Reactions, ICTP Trieste, Italy, 4-8 February 2008, D. Filges, S. Leray, Y. Yariv, A. Mengoni, A. Stanculescu, and G. Mank Eds., IAEA INDC(NDS)-530, Vienna, August 2008, p181. http://www-nds.iaea.org/reports-new/indc-reports/indc-nds/indc-nds-0530.pdf
[7] Leray S *et al.*, 2011 Journal of the Korean Physical Society, Vol. 59, No. 2, August 2011, p. 791.
[8] http://www-nds.iaea.org/spallations.
[9] Hendricks J S et al., 2005 "MCNPX EXTENSIONS VERSION 2.5.0", Los Alamos National Laboratory Report LA-UR-05-2675
[10] Agostinelli S et al. 2003 Nucl. Instrum. Meth. A 506 250 – 303
[11] Niita K, Matsuda N, Iwamoto Y, Iwase H, Sato T, Nakashima H, Sakamoto Y and Sihver L, "PHITS: Particle and Heavy Ion Transport code System, Version 2.23", JAEA-Data/Code 2010-022 (2010)
[12] Mokhov N V and Striganov S I, MARS15 overview, Hadronic Shower Simulation Workshop, 2007 IP CONFERENCE PROCEEDINGS, Editors: Albrow, M; Raja, R, Vol. 896, 50.
[13] Schardt D et al., Tumor therapy with high-energy carbon ion beams, 2007 Nucl. Phys. A787 633c.
[14] Durante M and Kronenberg, A Ground-based research with heavy ions for space radiation protection, 2005 Adv Space Res. 35:180-184.
[15] James M R et al., Recent Enhancements in MCNPX: Heavy Ion Transport and the LAQGSM Physics Model, International Conference on Accelerator Applications 2005, Venice, Italy, August 29 - September 1
[16] Cugnon J *et al.*, submitted to Phys. Rev. C.
[17] David J C *et al.*, submitted to EPJA.
[18] A. Boudard, J. Cugnon, S. Leray and C. Volant, 2004 Nucl. Phys. **A 740**, 195.
[19] S. Leray *et al.*, Nucl. Instr. and Meth. in Physics Research B 268 (2010) 581
[20] G. Igo and B.D. Wilkins, 1963 Phys. Rev. 131, 1251
[21] A. Ingemarsson *et al.*, 2000 Nucl. Phys. **A 676**, 3.
[22] A. Ingemarsson *et al.*, 2001 Nucl. Phys. **A 696**, 3.
[23] http://www-nds.iaea.org/exfor/
[24] J.C. David *et al.*, 2010 Shielding Aspects of Accelerators, Targets and Irradiation Facilities - SATIF-10; Workshop Proceedings, Geneva, Switzerland 2-4 June 2010, OECD/NEA", p 413.
[25] Y. Tall et al., 2008 Proceedings of the International Conference on Nuclear Data for Science and Technology, April 22-27, 2007, Nice, France, Ed. O. Bersillon, F. Gunsing, E. Bauge, R. Jacqmin, and S. Leray, EDP Sciences p1069.
[26] W. B. Wilson, et al., "Status of CINDER'90 Codes and Data", 1998 Proc. 4th Workshop on Simulating Accelerator Radiation Environments, September 13-16, 1998, Knoxville, Tennessee, USA, pp. 69-79, Los Alamos National Laboratory Report LA-UR-98-361.
[27] A. Boudard, J. Cugnon, P. Kaitaniemi, S. Leray, D. Mancusi, "Simulation of light ion collisions from Intra Nuclear Cascade (INCL-Fermi Breakup) relevant for medical irradiations and radioprotection", 2010 Proc. Int. Topical Meeting on Nuclear Research Applications and Utilization of Accelerators 2009, Vienna, Austria, May 5-8, 2009.
[28] P. Kaitaniemi, A. Boudard, S. Leray,J. Cugnon, D. Mancusi, 2011 Progress in NUCLEAR SCIENCE and TECHNOLOGY, Vol. 2, pp.788-793.
[29] A. Heikkinen, P. Kaitaniemi, A. Boudard, "Implementation of INCL4 cascade and ABLA evaporation codes in GEANT4," 2008 J. Phys. Conf. Ser., 119, 032024.
[30] J.M. Quesada *et al.*, 2011 Progress in NUCLEAR SCIENCE and TECHNOLOGY, Vol. 2, pp.936-941.
[31] Folger G, Ivanchenko V N and Wellisch J P, 2004 Eur. Phys. J. A 21(3) 407–417
[32] T. Koi, "New Native QMD Code in Geant4", 2008 Proc. IEEE 2008 Nuclear Science Symposium, Dresden, Germany, Oct. 19-25, 2008.
[33] H. Sato *et al.*, 2001 Phys. Rev. C 64 034607.
[34] Y. Iwata *et al.*, 2001 Phys. Rev. C 64 034607.
[35] C. Zeitlin et al., 2008 Phys. Rev. C 77 (2008) 034605.
[36] Gunzert-Marx K, Iwase H, Schardt D and Simon R S, 2008 New J. Phys. 10 075003.
[37] Braunn B et al., this conference.
[38] Braunn B et al., 2011 Nucl. Instrum. Meth. B 269 2676 – 2684